

# Optimization design of magnetically suspended system for the BiVACOR total artificial heart

Nobuyuki Kurita<sup>a</sup>, Daniel Timms<sup>b</sup>, Nicholas Greatrex<sup>b</sup>, Matthias Kleinheyer<sup>b</sup>, Toru Masuzawa<sup>c</sup>

<sup>a</sup> Gunma University, 1-5-1 Tenjin, Kiryu, Gunma, JAPAN, nkurita@gunma-u.ac.jp

<sup>b</sup> Texas heart Institute, 6770 Bertner Avenue, Houston, Texas, USA, dtimms@texasheart.org

<sup>c</sup> Ibaraki University, 4-12-1 Nakanarusawa, Hitachi, Ibaraki, JAPAN, masuzawa@mx.ibaraki.ac.jp

**Abstract**— The BiVACOR device is a third generation rotary total artificial heart under development to treat end stage cardiovascular disease. Non-contact suspension and rotation of the impeller of the blood pump was achieved by a combination of a permanent magnet hybrid type magnetic bearing and an axial flux brush-less DC motor. Moreover, according to a series of animal trials, functionality of the proposed magnetic system in the total artificial heart application was clarified.

## I. INTRODUCTION

Due to the high rate of heart disease and shortage of donor hearts [1], there has been a longstanding interest to develop mechanical replacement for the heart. Recently, third generation rotary blood pumps of implantable size have shown considerable promise in this application [2]–[6]. These devices utilize magnetic or hydrodynamic bearings support the impeller which eliminates any mechanical contact. Therefore, the operational mechanical lifetime of these devices may exceed ten years.

The BiVACOR, third generation rotary total artificial heart (TAH) is under development to treat end stage cardiovascular disease [7], [8]. It utilizes the magnetic suspension system to not only reduce device wear, but to assist in automatically balancing left and right device outflows by utilizing virtual zero power control algorithms. This paper provides an insight into the TAH's magnetic system components, including the magnetic bearing and axial motor technologies, the resulting flow balancing performance when implemented in a chronic animal trial.

## II. EXPERIMENTAL DEVICE

### A. Total Artificial Heart

Figure 1 shows an exploded view of the BiVACOR TAH. The outer diameter and height of the device are approx. 60 mm and 70 mm, respectively. The device includes a set of left and right impeller vanes positioned on opposing sides of the rotor core to form double-sided centrifugal impeller. Active axial rotor suspension is achieved with three axial magnetic bearings and rotated via an axial flux motor. Although they are omitted in figure, three eddy current displacement sensors are arranged between the magnetic bearings to measure axial displacement.

Since the left and right impeller blades are inherently coupled to the common rotating rotor core, if rotational speed is slowed, the both of the outflow of the left and right pumps

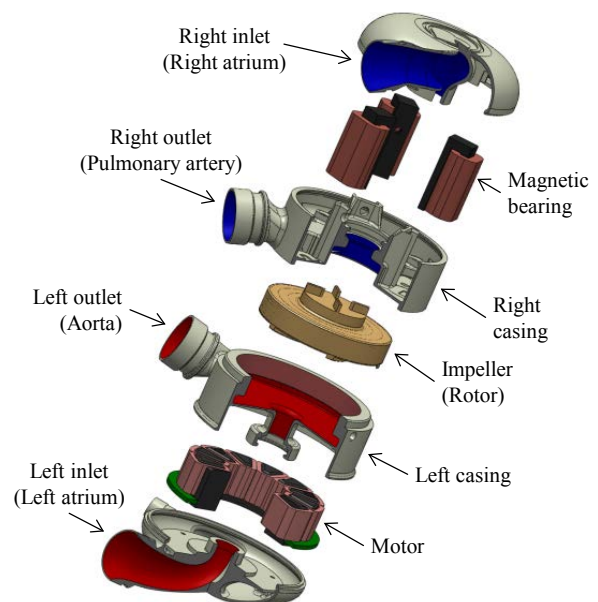


Figure 1. Schematic of developed magnetically levitated TAH

will be reduced simultaneously. However, to account for the required changes in relative left and right outflow, the magnetic bearing system can displace the impeller axially with in the pump cavity. This action simultaneously alters the efficiency of each semi-open impeller vane set in an inverse relationship. For example, a movement toward the left cavity will increase left out flow while reducing right outflow, and vice versa [7].

### B. Magnetically Levitation Rotation System

The magnetic bearing is composed of three horseshoe shaped electromagnets in the casing and two ring shape permanent magnets on the rotor to produce bias flux. These magnetic bearings are evenly spaced 120° apart; regulating axial displacement and tilt of the rotor impeller, depending on the feedback from the displacement sensor signals. Figure 2(a) shows the components of the magnetic bearing. The horseshoe shaped stator core has a coil winding on its one leg. Two ring shape permanent magnets (Inner ring PM and outer ring PM) are attached on the rotor disk as the bias PMs which produces bias flux at the airgap between the stator and the rotor. Figure 2 (b) and (c) shows the operating principle of the magnetic bearing for the position control mode. As mentioned above,

the bias flux path was generated by the bias PM as shown in the figure by the green dotted line. When the rotor was moved by the disturbance force, the displacement sensors detect the rotor movements and feedback the displacement signal to the PID controller. The PID controller applies adequate control current to the windings. Figure 2(b) shows operating principle in order to increase magnetic force. The flux density at the airgap is strengthened by the control flux shown by the orange solid arrow. In a contrasting situation, the airgap flux density is weakened by the negative control current in the Figure 2(c).

Figure 2(d) and (e) shows the operating principle for the zero power modes. When the rotor was moved by the disturbance force, the detected displacement signals are feedback the signal to the virtual zero power (VZP) controller which regulates the control current to be zero. As shown in Figure 2(d), when the disturbance force acts on the rotor downward, the rotor moves upward where the disturbance force and the permanent magnet attractive force are balanced. In a contrasting situation, when the disturbance force acts on the rotor upward, the rotor moves downward in order to weaken the airgap flux density as shown in Figure 2(e).

According to the VZP control, the distance of the rotor displacement  $D_R$  (m) depends on the strength of the disturbance force  $F_D$  (N) and the stiffness of the magnetic levitation system  $K_{MLV}$  (N/m) as shown in Equation (1).

$$D_R = \frac{F_D}{K_{MLV}} \quad (1)$$

In general zero-power control, the stiffness of the magnetic levitation system  $K_{MLV}$  is a constant value which is the difference between the magnetic bearing suspension force stiffness  $K_{MB}$  and the motor attractive force stiffness  $K_M$ . However, the magnetic bearing suspension force stiffness is controllable by the small constant control current of the electromagnets, i.e.  $\Delta K_E$ . By substituting  $K_{MB}$ ,  $K_M$  and  $\Delta K_E$  to Equation (1),  $D_R$  is expressed as follows.

$$D_R = \frac{F_D}{(K_{MB} + \Delta K_E) - K_M} \quad (2)$$

According to the Equation (2), the distance of the rotor displacement  $D_R$  is also controllable in VZP mode. In this paper, however, disturbance force which acts on the rotor is unmeasurable. Only the pressures (inlet and outlet pressure of both of left and right pumps) are measurable. Thus, we don't use disturbance force but disturbance pressure. Because the surface area of the impeller won't change, the force and the pressure essentially have the same implications in this paper.

The axial flux motor is composed of twelve stator poles and eight permanent magnets on the rotor as field magnets. It is operated as a permanent magnetic synchronous motor using back EMF to determine the rotor position. The left impeller is installed in the motor side airgap. Therefore, the airgap width between the surface of the stator pole and permanent magnet is very wide (3.4mm).

### C. Automatic Rotor Position Control

Systemic vascular resistance (SVR) and the pulmonary vascular resistance (PVR) are altered by various causes such as changes in posture, sneezing, exercise and so on. Decrease

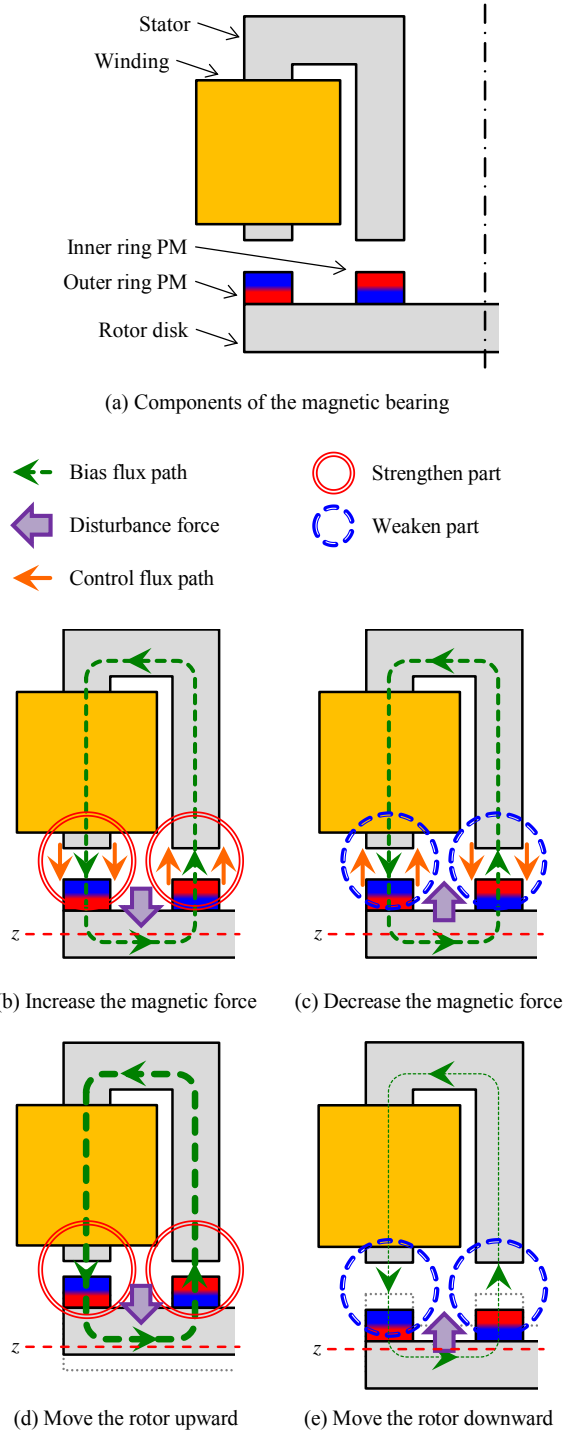


Figure 2. Operating principle of the magnetic bearing

of SVR results in an increase of left sided flow rate of the TAH. This causes a drop in the left atrial pressure (LAP) and the aortic pressure (AOP). If the LAP become below 0 mmHg, a suction event may occur. In order to avoid such an event, the rotor should move toward right side to reduce the pressure differential and thus outflow rate of the left pump. As previously described, to accommodate these required changes in flow rate and pressure, the rotor axial position should be varied by the magnetic bearing. Automatic rotor position compensation is achieved by the VZP. When the AOP and the

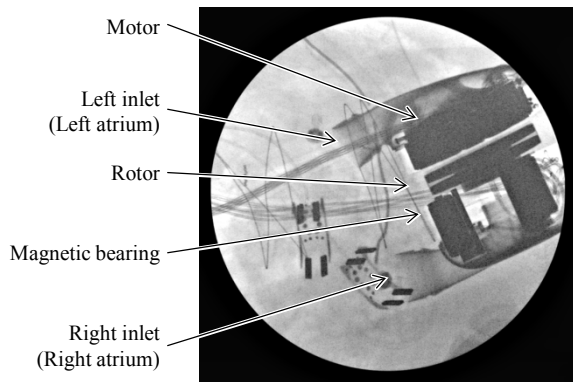


Figure 3. Angiogram of the BiVACORE during animal trial

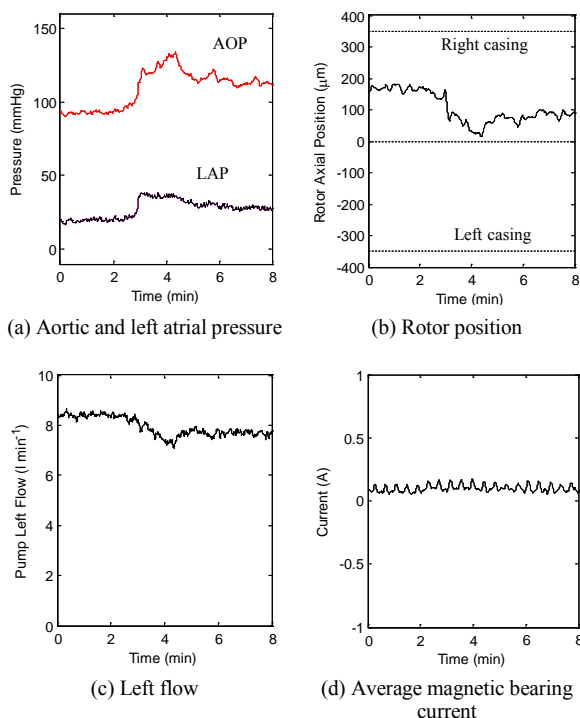


Figure 4. Results of the chronic animal trial

LAP decrease, the hydraulic force from left side to right side also decreases. Consequently VZP moves the rotor toward right side to balance the hydraulic force and the magnetic force of the magnetic system. An increase of SVR causes an increase of the LAP. In order to decrease the LAP and also increase the right atrium pressure (RAP) and pulmonary artery pressure (PAP), the rotor should be moved toward left side. When the LAP increased, the hydraulic force from left side to right side also increases. Then VZP automatically responds to move the rotor toward left side.

Although this controller is designed to normally operate with a target current of 0 A, the set point of the current control can be modified to alter the rotor's steady state position. This can be used by a user to improve the balancing of the TAH in particular patients and scenarios.

### III. EXPERIMENTAL RESULT

In order to verify the functionality of the developed BiVACOR TAH, a recovery trial was completed. An 87.5 kg male calf was supported for more than 2 days. Figure 3 shows

angiogram of the BiVACOR TAH during the animal trial. According to the figure, it is clear that the stable magnetic levitation was achieved by magnetic bearings and the axial flux motor. In the position control mode, the axial directional rotor position movement of  $\pm 0.3\text{mm}$  was also achieved. Moreover, the stable levitated rotation was also achieved in the objective speed range from  $1,800\text{ min}^{-1}$  to  $2,800\text{ min}^{-1}$ . In addition, the pulsatile speed control ability was also confirmed, in order to produce washout flow to prevent thrombus formation within the device.

Figure 4 shows the results of an event in which the calf returned to the sitting position after standing for approximately 15 minutes. As shown in Figure 4(a), when the sit-down event occurs, at  $t = 3\text{ s}$ , the AOP and LAP rise causing the hydraulic force acting on the rotor to increase towards the right casing. The VZP controller acts to resolve this force and moves the rotor  $130\text{ }\mu\text{m}$  towards the left of the pump casing increasing the relative efficiency of the left pump (Figure 4 (b)). Approximately 5 seconds after the event occurred the system stabilizes with a steady state rotor position of approximately  $70\text{ }\mu\text{m}$  towards the left casing from its pre-event position. The change in posture caused a steady state increase to the SVR resulting in a new flow rate of  $7.5\text{ l/m}$  which is  $0.5\text{ l/m}$  lower than before the event (Figure 4 (c)). The AOP and LAP increased by  $20\text{ mmHg}$  and  $7\text{ mmHg}$  respectively. As mentioned above, the stiffness of the rotor movement versus disturbance pressure is controllable by the small constant control current of the electromagnets. The average magnetic bearing current remained close to its set point of  $0.1\text{ A}$  throughout the event (Figure 4 (d)) with the periodic breathing events clearly visible on the signal.

### IV. DISCUSSION

The performance of the magnetic system was sufficient to maintain stable levitation and rotation at speeds required for TAH support. The VZP controls the rotor axial position automatically to compensate flow rate and pressure to avoid suction events.

By the VZP, the rotor moves axially due to the pressure difference of the left and right pump. The pressure acting on the rotor can be calculated as follows.

$$\Delta P = (AOP - LAP) - (PAP - RAP)$$

The pressure difference before and after the stand-up event was  $\Delta P = 9\text{ mmHg}$ . The change of rotor displacement was  $70\text{ }\mu\text{m}$ . Therefore, the system stiffness is  $7.8\text{ }\mu\text{m/mmHg}$ . This system stiffness was achieved by configuring the magnetic suspension system to have a low magnetic stiffness. The magnetic airgap of the motor and magnetic bearings were chosen to be large to lower the magnetic stiffness while maintaining the location of the magnetic zero point. The resulting system has yielded appropriate system stiffness; however the larger airgaps reduce the efficiency and performance of the motor and magnetic bearings. To improve the power consumption of the device changes to the motor, such as increasing the winding number and pole configuration will be investigated, whilst trying to maintain the desired stiffness demonstrated in this system.

The axial flux motor was driven by sensorless position detection using back EMF. It achieved pulsatile speed control, in order to produce washout flow to prevent potential

thrombus formation. However, wide magnetic airgaps and cyclic speed change leads to a reduction of efficiency. The energy consumption of the implantable TAH should be as small as possible. Therefore, efficiency of the axial flux motor should be improved by an increase of the winding number and different configuration of motor poles.

## V. CONCLUSION

A magnetic system for the BiVACOR TAH was designed and developed. The magnetic levitation system enables axial movement of the rotor during rotation. According to a chronic animal trial, stable levitated rotation was achieved in the objective speed range of the designed blood pump. The VZP indicated good automatic rotor position control performance in response to variations in pressure, and thus effectively balanced left/right outflows. Moreover, the trial clarified the functionality of the BiVACOR TAH.

## REFERENCES

- [1] American Heart Association, "Heart disease and stroke statistics – 2009 update", A report from the American Heart Association Statistics Committee and Stroke Statistics Subcommittee (2009)
- [2] Peter A. Watterson, John C. Woodard, Victor S. Ramsden and John A. Reizes, "Ventr Assist Hydrodynamically Suspended, Open, Centrifugal Blood Pump", *Artificial Organs*, Volume 24 Issue 6, pp. 475-477 (2001)
- [3] Toru Masuzawa, Shiroh Ezoe, Tsuyoshi Kato and Yohji Okada, "Magnetically Suspended Centrifugal Blood Pump with an Axially Levitated Motor", *Artificial Organs*, Volume 27 Issue 7, Pages 631-638 (2003)
- [4] Hideo Hoshi, Tadahiko Shinshi and Setsuo Takatani, "Third-generation Blood Pumps With Mechanical Noncontact Magnetic Bearings", *Artificial Organs*, Volume 24 Issue 6, pp. 324-338 (2006)
- [5] Hideyuki Fumoto, David J. Horvath, Santosh Rao, Alex L. Massiello, Tetsuya Horai, Tohru Takaseya, Yoko Arakawa, Nicole Mielke, Ji-Feng Chen, Raymond Dessoiffy, Kiyotaka Fukamachi and Leonard A. R. Golding, "In vivo acute performance of the Cleveland Clinic self-regulating, continuous-flow total artificial heart", *The Journal of Hert and Lung Transplantation*, Vol. 29, No. 1, pp. 21-26 (2010)
- [6] O.H. Frazier and William E. Cohn, "Continuous-Flow Total Heart Replacement Device -Implanted in a 55-Year-Old Man with End-Stage Heart Failure and Severe Amyloidosis-", *Tex Heart Institute Journal* Vol. 39, No. 4, pp. 542-546 (2012)
- [7] Nobuyuki Kurita, Daniel Timms, Nicholas Greatrex, Toru Masuzawa, "Axial Magnetic Bearing Development for the BiVACOR Rotary BiVAD/TAH", *The proceedings of the 11th International Symposium on Magnetic Bearings*, pp. 217-224 (2008)
- [8] Nicholas A. Greatrex, Daniel L. Timms, Nobuyuki Kurita, Edward W. Palmer and Toru Masuzawa, "Axial Magnetic Bearing Development for the BiVACOR Rotary BiVAD/TAH", *IEEE Transactions on Biomedical Engineering*, Vol. 57, No. 3, pp 714-721 (2010)